



Contents lists available at ScienceDirect

Mechanical Systems and Signal Processing

journal homepage: www.elsevier.com/locate/jnlabr/ymssp

Application of regularization dimension to gear damage assessment

Zhipeng Feng^{a,b,*}, Ming J. Zuo^b, Fulei Chu^c^a Institute of Vehicular Engineering, University of Science and Technology Beijing, Beijing 100083, China^b Department of Mechanical Engineering, University of Alberta, Edmonton, Alberta, Canada T6G 2G8^c Department of Precision Instruments, Tsinghua University, Beijing 100084, China

ARTICLE INFO

Article history:

Received 15 October 2008

Received in revised form

19 August 2009

Accepted 23 August 2009

Keywords:

Gear

Localized damage

Fractal dimension

Regularization dimension

Gaussian kernel

ABSTRACT

Fractal dimension provides a measure of the complexity of a dynamic system, and contains the health information of a machine. The basics of regularization dimension and the effects of Gaussian kernel parameters on the regularization of a signal are introduced. Regularization dimension has advantages over other fractal dimensions because the scale-independent range can be selected according to the signal frequency components of interest. Experimental gearbox vibration signals are analyzed by means of spectral analysis firstly, and then according to the spectral structure, the scale-independent range is selected for computing the regularization dimension, which increases monotonically with increasing gear damage degree. Comparison with correlation dimension and kurtosis shows the advantages of regularization dimension in assessing the localized gear damage.

© 2009 Elsevier Ltd. All rights reserved.

1. Introduction

Gears, as important mechanisms for transmitting power or rotation, play an important role in many sorts of machineries. Smooth operation and high efficiency of gears are necessary for the normal running of machineries. Therefore, gear damage assessment is an important topic in the field of condition monitoring and fault diagnosis.

Most gear faults are due to localized gear damage, such as tooth wear, cracks, scoring, spalling, chipping, and pitting [1]. With such flaws existing on gears, progressive damage will occur and ultimately result in gear tooth breakage. Therefore, localized damage assessment is of great practical importance to the monitoring and diagnosis of gears.

Many statistical metrics have been applied to gear damage assessment, such as the root mean square, crest factor, kurtosis, FM0, FM4, FM4*, M6, M6A, M6A*, NA4, NA4*, NB4, NB4*, S_z , S_r , etc. [1]. Most of these metrics study gear vibration signals from the viewpoint of statistics. They provide a measure of vibration intensity or characterize the statistical properties of vibration. However, they cannot give an insight into the gear dynamic system generating the vibration signals.

Usually, the dynamic system of a gearbox exhibits nonlinearity due to the intrinsic complicated motion, time-varying running condition, and fault-induced factors. The above-mentioned statistical metrics of vibration signals have inherent shortcomings in investigating the nonlinearity of a gear dynamic system.

Fractals are a promising approach to nonlinear dynamics [2–6]. The word ‘fractal’ was coined by Mandelbrot [2] to describe objects that are too irregular to fit into a traditional geometrical setting. A set is defined (by Falconer [3]) in the same way as biologists regard the definition of ‘life’ as a fractal if it is characterized by the following properties: (1) it has a

* Corresponding author at: Institute of Vehicular Engineering, University of Science and Technology Beijing, Beijing 100083, China.

Tel.: +86 10 62332865; fax: +86 10 82381628.

E-mail addresses: zhipeng.feng@yahoo.com.cn (Z. Feng), ming.zuo@ualberta.ca (M.J. Zuo), chufu@mail.tsinghua.edu.cn (F. Chu).

fine structure, i.e. details on arbitrarily small scales; (2) it is too irregular to be described in traditional geometrical language, both locally and globally; (3) it often has some form of self-similarity, perhaps approximate or statistical; (4) usually, its ‘fractal dimension’ (defined in some way) is greater than its topological dimension; and (5) in most cases of interest it is defined in a very simple way, perhaps recursively. The fractal dimension measures quantitatively the complexity and irregularity of a fractal. In dynamics, it is a useful tool to characterize the nonlinearity and complexity of a dynamic system [2–6]. So far, several different definitions have been proposed, such as the capacity dimension, information dimension, and correlation dimension (refer to [5,6] for their definitions). They are all based on the same idea—‘measurement at a scale δ ’.

Theoretically, when the condition of a machine changes, its dynamic parameters such as the mass, stiffness, and/or damping will also change, and accordingly result in a variation of the vibration response in terms of complexity. Namely, the vibration signal complexity of a machine under faulty condition is different from that under healthy condition. In this sense, fractal dimension contains the running-condition information of a machine, and can be employed to extract features from vibration signals for condition assessment [6–11].

Recently, fractal dimension has been studied in the field of machinery monitoring and diagnosis. Logan and Mathew [7,8] studied the effect of relevant parameters (such as data length and parameters in state space reconstruction of time series) on the computation of correlation dimension based on state space reconstruction of time series, and applied the correlation dimension to extract features for damage detection of rolling element bearings. Jiang et al. [9] discussed the influence of sample size and noise level on the computational precision of correlation dimension, and used the correlation dimension to identify the running condition of a gearbox. Wang et al. [10] researched the application of some nonlinearity analysis methods, including the pseudo-phase portrait, singular spectrum, and correlation dimension, for monitoring and diagnosis of rotating machinery, and they found that the correlation dimension can be used to indicate the number of state variables dominating the dynamic response of a nonlinear system. Yang et al. [11] applied fractal dimensions, including the capacity dimension, information dimension, and correlation dimension, to extracting features from vibration signals for damage pattern classification of rolling element bearings.

The researches mentioned above demonstrate the effectiveness of fractal dimension in assessing the condition of machinery. However, most of these researches focus on the common fractal dimensions obtained by the box-counting method, such as the correlation dimension, capacity dimension, and/or information dimension. The computational precision of these fractal dimensions is affected by many factors. For example, the state space reconstruction of time-series-based correlation dimension is affected by the embedding dimension of reconstructed state space, intra-vector spacing, inter-vector spacing, and correlation integral counting offset; moreover, it is difficult to select a scale-independent range when computing the fractal dimension, especially when a signal is contaminated by noise [6–11].

Regularization dimension [12,13] is a new definition of fractal dimension. Inspired by the motivation of fractal dimension, it is defined in a way to measure the irregularity of a signal. Signals are smoothed (or regularized) by convolution with Gaussian kernels, the relationship between the length of the smoothed signal and the Gaussian kernel width is studied, and thereby the fractal dimension is obtained. If the original signal is fractal, it has infinite length, while all smoothed versions have finite length. When the width of Gaussian kernel tends to 0, the smoothed version approaches the original signal, and its length tends to infinity. The regularization dimension measures the speed at which the length of a smoothed signal converges to infinity when the width of Gaussian kernel approaches 0.

In general, regularization dimension coincides with those obtained by the usual box-counting method, but it is more precise and more robust because the smoothed signals are constructed adaptively, and the width of Gaussian kernel can vary in very small steps, whereas box sizes have to undergo sudden changes [12,13].

In this paper, regularization dimension is applied to assess the localized damage of gears. In Section 2, the concept of fractal dimension, and the basics of regularization dimension and Gaussian kernel are introduced. In Section 3, regularization dimension is applied to analyze gearbox vibration signals. Its effectiveness is verified by two kinds of experimental datasets: one is from an experiment of localized gear damage including chipping, tooth breakage, and their combination, and the other one is from a run-to-failure test of a gearbox. It is found that regularization dimension outperforms correlation dimension and kurtosis. Its advantages lie in the fact that the scale-independent range can be selected according to the signal frequency components of interest, and the risk of information loss caused by signal preprocessing (e.g., denoising prior to computing correlation dimension), as well as the complicated state space reconstruction of time series, can be avoided, so that the real gear damage degree can be revealed more accurately. Finally, a conclusion is summarized in Section 4.

2. Regularization dimension

2.1. Fractal dimension

Fractal dimension is an important parameter to study fractals. It might be an integer or a fraction. Mandelbrot [2] proposed the concept of fractals and fractal dimension when he studied the problem ‘how long is the coastline of Britain?’ If the coastline is measured at a unit scale ε , and the number of total segments is $N(\varepsilon)$, then it is taken for granted that the length of coastline $L(\varepsilon)=N(\varepsilon)\varepsilon$, and $L(\varepsilon)$ approaches the true length as the unit scale ε becomes smaller and smaller. But this

is not true. With the scale ε becoming smaller and smaller, e.g., till the level of molecule and atom, more and more, even infinite, details will be taken into account, so $L(\varepsilon)$ also becomes progressively larger and even tends to infinity. The coastline should be measured or compared by a metric that is irrelative to scale ε . Actually, $N(\varepsilon)\varepsilon^D = \text{constant}$, where D is a constant and is usually not an integer. Mandelbrot named the parameter D as the fractal dimension, and considered it a useful metric to characterize coastlines.

So far, many definitions of fractal dimension have been proposed, but a general and strict mathematical definition has not been given. All the definitions are based on the idea of 'measurement at scale δ '. For each δ , a set F is measured in such a way that irregularities of size less than δ are ignored. If the measurement $M_\delta(F)$ obeys a power law as $\delta \rightarrow 0$ of the form

$$M_\delta(F) \sim c\delta^{-s}$$

for constants c and s , then F has a fractal dimension s , and it can be estimated as

$$s = \lim_{\delta \rightarrow 0} \frac{\ln M_\delta(F)}{-\ln \delta},$$

when the limit exists.

Box-counting method is commonly used to compute the fractal dimension. It uses small 'boxes' with an adjustable size ε to cover a fractal, counts the number of boxes $N(\varepsilon)$, and defines the fractal dimension as

$$d = -\lim_{\varepsilon \rightarrow 0} \frac{\ln N(\varepsilon)}{\ln \varepsilon},$$

when the limit exists.

Moon [5] summarized a general computing equation of fractal dimension based on the box-counting method. The capacity, information, and correlation dimensions can be estimated by the general equation

$$d(q) = \lim_{\varepsilon \rightarrow 0} \lim_{q_i \rightarrow q} \frac{1}{q_i - 1} \frac{\ln \sum_{i=1}^{N(\varepsilon)} P_i^{q_i}(\varepsilon)}{\ln \varepsilon}, \quad (1)$$

when the limit exists, where ε is the size of a covering box, $N(\varepsilon)$ the number of boxes used to cover the signal, and $P_i(\varepsilon)$ the probability for a point to lie in the covering box, which can be computed as the proportion of the signal points that lie in the i th covering box. When $q=0$, 1, and 2, $d(q)$ becomes an estimate of capacity dimension, information dimension, and correlation dimension, respectively.

2.2. Regularization dimension

Regularization dimension is defined in a way different from that based on the box-counting method. Its principle is as follows [12,13].

Let s denote a signal, and s_σ the signal smoothed by convolution with a Gaussian kernel g_σ of kernel width σ (which will be introduced in Section 2.3):

$$s_\sigma = s * g_\sigma. \quad (2)$$

Assume that the signal s is so irregular that it has infinite length. When it is smoothed with a Gaussian kernel g_σ of width $\sigma > 0$, it becomes more regular, and has a finite length l_σ . Furthermore, when the width σ tends to zero, the Gaussian kernel g_σ tends to an impulse, so the smoothed signal s_σ approximates the original signal s , and its length l_σ approaches infinity. The regularization dimension measures the speed for the length of the smoothed signal l_σ to converge to infinity when the width of Gaussian kernel σ tends to zero. Formally, the regularization dimension is defined as

$$d = 1 - \lim_{\sigma \rightarrow 0} \frac{\ln l_\sigma}{\ln \sigma}, \quad (3)$$

when the limit exists.

For a real signal, the logarithm of the smoothed signal length $\ln l_\sigma$ may not vary linearly with respect to the logarithm of the Gaussian kernel width $\ln \sigma$. Usually, a range of interest in which the graph of $\ln l_\sigma - \ln \sigma$ is approximately linear is determined as the scale-independent range. Then a linear regression of $\ln l_\sigma$ versus $\ln \sigma$ is made in this range, and the slope of the regression line is used to estimate the regularization dimension according to Eq. (3).

2.3. Gaussian kernel

The smoothing or regularization of a signal with a Gaussian kernel is to convolve the signal with a Gaussian kernel, and it is equivalent to filtering the signal with a Gaussian filter. The parameters of Gaussian kernels should be properly selected when computing the regularization dimension.

The family of a 1-D Gaussian and its n th order derivatives with a kernel width σ and centered at the origin can be defined as [14,15]

$$g_{\sigma}^{(0)}(t) = \exp\left(-\frac{t^2}{2\sigma^2}\right), \tag{4a}$$

$$g_{\sigma}^{(n)}(t) = \frac{d^{(n)}}{dt^{(n)}} g_{\sigma}^{(0)}(t). \tag{4b}$$

The Fourier transform of a Gaussian and its derivatives are also Gaussians [14,15], i.e.

$$G_{\sigma}^{(0)}(\omega) = \sigma \exp\left(-\frac{\sigma^2 \omega^2}{2}\right), \tag{5a}$$

$$G_{\sigma}^{(n)}(\omega) = (-j\omega)^n G_{\sigma}^{(0)}(\omega). \tag{5b}$$

Their spectral modes center at

$$\omega_{\sigma}^{(n)} = \frac{\sqrt{n}}{\sigma}. \tag{6}$$

(Note that ω is the angular frequency in the unit of rad/s. It differs from the frequency f in the unit of Hz by a factor of $F_s/2\pi$, i.e. $f=F_s\omega/2\pi$, where F_s is the sampling frequency for a digital signal.) The kernel width σ defines the extent of these functions in the time domain, as well as the bandwidth in the frequency domain (within the extent and bandwidth, the amplitude of neither the waveform nor the spectrum is negligible).

From Eqs. (4)–(6), the effect of Gaussian kernel width and derivative order on the amplitude–frequency characteristics can be deduced; both the center frequency and bandwidth of spectral mode are inversely proportional to the kernel width, so if the derivative order is fixed, when the kernel width increases, both the center frequency and bandwidth of spectral mode decrease; the center frequency of spectral mode is directly proportional to the square root of derivative order, so if the kernel width is fixed, when the derivative order increases, the center frequency of spectral mode also increases.

In order to control the relative amplitude of Gaussians at both ends in time domain and the relative amplitude of sidelobes at both sides of center frequency in frequency domain, as well as the increment of Gaussian kernel width and center frequency with an increase of time support, usually an attenuation coefficient is used, and the Gaussian kernel width is modified as [12,13]

$$\sigma = \frac{i - 1}{2\sqrt{\alpha \ln 10}}, \tag{7}$$

where i defines the time support of Gaussian kernel, $i=2, 3, \dots$ (within these time supports, the amplitude of Gaussian is not negligible); α is the attenuation coefficient, usually its default value is set to $\alpha=2$ [12,13].

Fig. 1 illustrates the effect of kernel width on the spectrum of a 5th order Gaussian derivative with the attenuation coefficient $\alpha=2$, and the time support $i=9, 41$, and 73 . Fig. 2 illustrates the effect of derivative order (0th, 9th, and 18th orders) on the spectrum of a Gaussian with a time support of 19 and attenuation coefficient of 0.5.

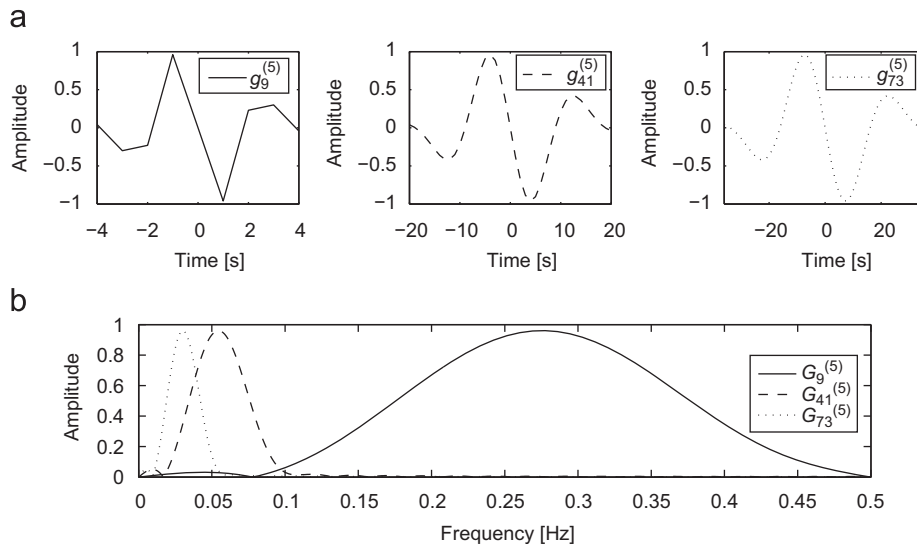


Fig. 1. Gaussians of fixed derivative order ($n=5$) and attenuation coefficient ($\alpha=2$) but different kernel widths: (a) waveform and (b) spectra.

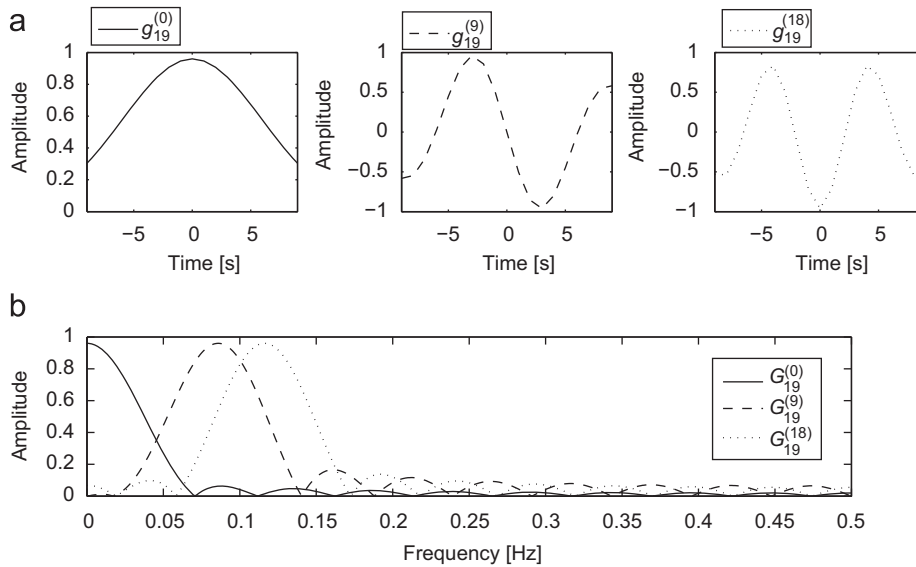


Fig. 2. Gaussians of fixed kernel width ($i=19$) and attenuation coefficient ($\alpha=0.5$) but different derivative orders: (a) waveform and (b) spectra.

From Fig. 1, it can be observed that with fixed derivative order n and attenuation coefficient α , the larger the time support i (accordingly kernel width σ), the smaller the center frequency and bandwidth of spectral mode. According to Eq. (7), the time support i is any integer larger than 1, usually it ranges from 2 to $(2/3)N$ (N is the number of data points) [12,13].

From Fig. 2, it can be observed that with fixed time support i (accordingly kernel width σ) and attenuation coefficient α , the larger the Gaussian derivative order n , the larger the center frequency of spectral mode. Based on Eq. (6), it can be deduced that the larger the Gaussian derivative order n , the larger the spacing between adjacent spectral modes of different kernel widths, so more frequency components between adjacent spectral modes may be missed (because when a signal is smoothed (filtered) by two Gaussian kernels of different kernel widths, the frequency components within the spacing between two spectral modes do not lie in either passband of the two Gaussian filters, and they will be filtered out). In this sense, a smaller derivative order n is desired, but order 0 is not the best, because when the derivative order of Gaussian n is 0, the center frequency of its spectral mode always equals 0; accordingly the Gaussian becomes a low-pass filter with its cut-off frequency determined by the kernel width, so lower frequency components always dominate the filtered signal, whereas higher frequency components cannot be highlighted. Based on the above analysis, and following the suggestion given in [12,13], the first order Gaussian derivative is used to regularize/filter the signals in this paper.

From the comparison between Figs. 1 and 2, it can be found that the larger the attenuation coefficient α , the smaller the sidelobes in the spectra. In order to suppress the sidelobes, a larger attenuation coefficient is desired, but a very large one may result in a large center frequency of the spectral mode that may be larger than Nyquist frequency (half the sampling frequency), so that some lower frequency components may not be covered after regularization. In this paper, the attenuation coefficient α is set to the default value of 2, following the suggestion given in [12,13].

Regularization dimension is determined by the relationship between the length of smoothed signal and the Gaussian kernel width, which is mainly determined by time support. Therefore, in the algorithm to compute the regularization dimension of a signal, the derivative order of Gaussian kernels and attenuation coefficient are fixed, while the time support is changed in a specified range. So the smoothing of the signal, i.e. convolving it with Gaussian kernels of different kernel widths, is equivalent to filtering the signal with a filter series of different center frequencies and different effective pass bandwidths. Only the frequency components within the passband of Gaussian filters contribute to the regularization dimension. This provides a guide to select the scale-independent range, i.e. it can be selected according to the frequency components of interest.

3. Gearbox vibration signal analysis

In order to assess the condition of gearboxes using regularization dimension, both the parameters of Gaussian kernels and the scale-independent range for computing regularization dimension should be properly selected according to the spectral structure of the vibration signals. Firstly, the gearbox vibration signals are analyzed by means of power spectral analysis, to find the principal frequency components. Then, regularization dimensions in a range that corresponds to the frequency band of interest are computed for assessing the gearbox condition.

3.1. Localized gear damage assessment

Most gear faults are due to localized gear damage, such as tooth chipping and breakage. In this section, the vibration signals of a gearbox with localized damage, which includes chipped gear, broken gear, or their combination, are analyzed.

3.1.1. Specification of experimental system

Gear tooth chipping, breakage, and their combination are introduced to the gears in a gearbox to simulate localized gear damage [16]. The experimental system consists of a Spectra Quest gearbox dynamics simulator, a DSP SigLab vibration analyzer, two ICP accelerometers, two signal amplifiers, and a laptop computer, as shown in Fig. 3.

The gearbox contains six gears on three shafts, wherein gears 1 and 1', as well as gears 4 and 4', can slide on shafts 1 and 3, so as to mesh with gears 2 and 3, respectively (see Table 1 for the specifications of gears and their health conditions, and Fig. 4 for the actual damage of gears 1' and gear 4'), and to simulate healthy and faulty conditions:

- (1) all normal gears are in mesh, i.e. gear 1 meshes with gear 2, and 3 with 4;
- (2) the chipped gear 1' meshes with gear 2, and 3 with 4;
- (3) the broken gear 4' meshes with gear 3, and 1 with 2; and
- (4) the chipped gear 1' meshes with gear 2, and the broken gear 4' meshes with gear 3.

The two ICP accelerometers are mounted on the gearbox casing with studs, wherein accelerometer 1 is mounted on the input side of the gearbox, and accelerometer 2 on the output side.

The input shaft, shaft 1, is driven by the motor at a speed of 600 rpm, and the output shaft, shaft 3, is applied with a load of 2.443 Nm by the brake. The characteristic frequencies of shafts, gears, and rolling element bearings are summarized in Tables 2 and 3.

The vibration signals are collected at a sampling frequency of 2560 Hz, and 8192 points of data are recorded for each signal. The signals last 3.2 s, which covers 32 revolutions of shaft 1, 10.7 revolutions of shaft 2, and 17.8 revolutions of shaft

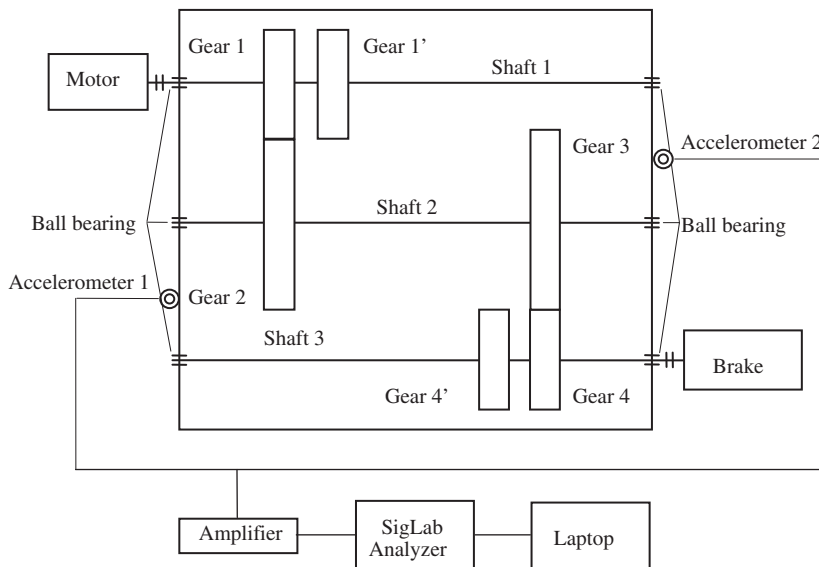


Fig. 3. Gearbox experimental system.

Table 1

Specification of gears.

Gear	Number of teeth	Damage
Gear 1	16	Normal
Gear 1'	16	One tooth is chipped
Gear 2	48	Normal
Gear 3	40	Normal
Gear 4	24	Normal
Gear 4'	24	One tooth is missing

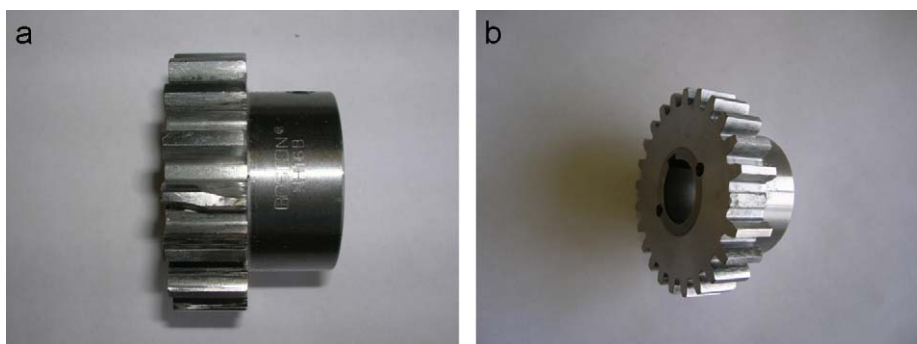


Fig. 4. Photos of chipped and broken gears: (a) tooth chipping of gear 1' and (b) tooth breakage of gear 4'.

Table 2

Characteristic frequencies of shafts and gears.

Rotating frequency of shaft 1	Rotating frequency of shaft 2	Rotating frequency of shaft 3	Meshing frequency of gear 1/1'	Meshing frequency of gear 3 and 4/4'
10 Hz	3.333 Hz	5.556 Hz	160 Hz	133.333 Hz

Table 3

Characteristic frequencies of rolling element bearings.

Bearing supporting	Ball pass frequency inner race (Hz)	Ball pass frequency outer race (Hz)	Fundamental train frequency (Hz)	Ball spin frequency (Hz)
Shaft 1	80.180	45.808	6.544	61.064
Shaft 2	26.724	15.268	2.181	20.353
Shaft 3	44.548	25.451	3.636	33.927

3. In order to reveal the dynamics of gears, the signals should cover at least one full revolution of each gear. Therefore, the signals collected are long enough to investigate the gearbox dynamics.

3.1.2. Spectral analysis

The waveforms and power spectra of the gearbox vibration signals (from accelerometer 2) under four conditions, i.e. when normal gears, chipped gear, broken gear, and chipped and broken gears are in meshing, are shown in Fig. 5.

From the power spectra, it can be seen that most of the signal energy is distributed in the frequency band 200–530 Hz. The peaks in this band correspond to harmonics of the gear meshing frequencies, or compound frequencies of gear rotating frequencies and meshing frequencies. Some sideband components exist on both sides of the peaks.

In the lower frequency band 0–200 Hz, a peak appears around 68 Hz. This frequency component is possibly produced by the vibration of bearings supporting the three shafts (refer to Table 2 for the characteristic frequencies of the bearings), because it approximately equals the second-order harmonic of the ball spin frequency of the bearing supporting shaft 3 ($2 \times 33.927 = 67.854$ Hz), or the compound frequency of the fundamental train frequency and the ball spin frequency of the bearing supporting shaft 1 ($6.544 + 61.064 = 67.608$ Hz).

3.1.3. Regularization dimension analysis

The gearbox vibration signals under the four types of condition are analyzed using the FracLab toolbox. When computing the regularization dimensions, the Gaussian derivative order is fixed to $n=1$, the attenuation coefficient is set to the default value $\alpha=2$, and the time support i ranges from 2 to 52, i.e. $i=2, 3, \dots, 52$. According to Eqs. (6) and (7), the spectral mode center of corresponding Gaussian kernels ranges from 34.3 to 1748.7 Hz, so that all the principal frequency components in the signals are covered.

The logarithm of the signal length $\ln l_\sigma$ versus the logarithm of the Gaussian kernel width $\ln \sigma$ is shown in Fig. 6. From a global point of view, $\ln l_\sigma$ does not vary linearly with respect to $\ln \sigma$, but from a local point of view, the graph of $\ln l_\sigma - \ln \sigma$ can be considered to be piecewise linear, e.g., in the range $[-0.3581, 0.7405]$ and $[0.7405, 1.4877]$ for $\ln \sigma$, the graph of $\ln l_\sigma - \ln \sigma$ has a linear trend, and is nearly scale independent. According to Eq. (6), they correspond to the frequency bands $[194, 583]$ and $[92, 194]$ Hz, respectively.

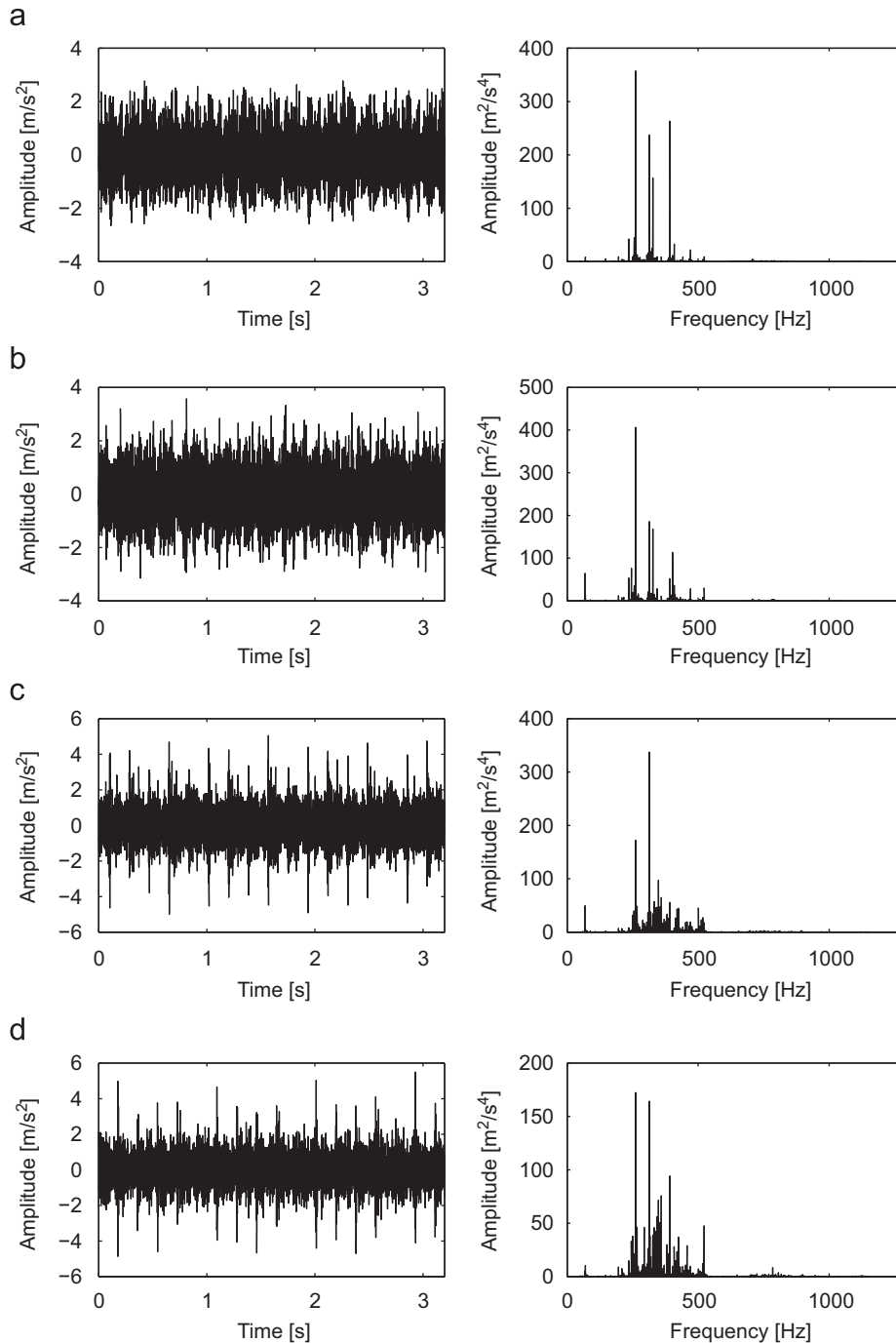


Fig. 5. Gearbox vibration signal waveforms (left) and power spectra (right): (a) normal gears; (b) chipped gear; (c) broken gear; and (d) chipped and broken gears.

As found in Section 3.1.2, most of the signal energy is distributed in the frequency band 200–530 Hz, and the dominant and prominent frequency components correspond to the harmonics of gear meshing frequencies, the compound frequencies of gear rotating frequencies and meshing frequencies, and the sidebands. Therefore, this frequency band is useful to reveal the gear damage. This frequency band is within the interval [194, 583] Hz, which corresponds to the range [4, 10] for the time support i and the range $[-0.3581, 0.7405]$ for the logarithm of the Gaussian kernel width $\ln \sigma$. In this range, the graph of $\ln l_\sigma - \ln \sigma$ is nearly linear, which means it is nearly scale independent, so it is used to compute the regularization dimension for assessing the gear condition.

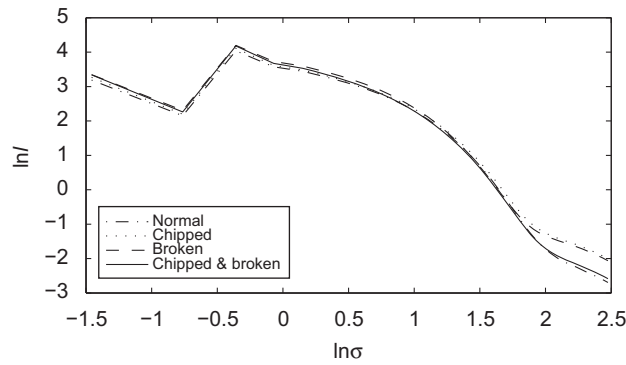


Fig. 6. Graph of $\ln l - \ln \sigma$.

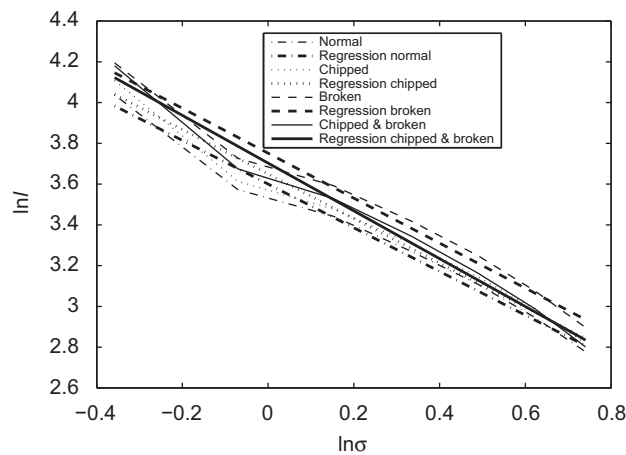


Fig. 7. Least squares regression.

Table 4
Fractal dimensions and kurtosis of gear vibration signals.

Gear condition	Normal	Chipped	Broken	Chipped and broken
Regularization dimension	2.0716	2.0913	2.1033	2.1723
Correlation dimension	3.9059	3.6320	4.7714	3.6755
Kurtosis	2.8344	2.9048	4.4354	4.4716

In the frequency band [92, 194] Hz corresponding to the interval [0.7405, 1.4877] for $\ln \sigma$, there is no prominent peak. It has no relevant information indicating the gear status. So the interval [0.7405, 1.4877] for $\ln \sigma$ is not used to calculate the regularization dimension, although it is nearly scale independent too.

By means of least squares error linear regression, a line can be found to fit the graph of $\ln l - \ln \sigma$ in a specific range, and its slope will be used to determine the regularization dimension. Fig. 7 shows the zoomed-in graph of $\ln l - \ln \sigma$ in the range [-0.3581, 0.7405] for $\ln \sigma$ and the corresponding least squares regression.

The regularization dimensions of the gearbox vibration signals under the four conditions are listed in Table 4, and their variation versus the damage degree is shown in Fig. 8, where damage degree 0 represents the condition that all the normal gears are in meshing, 1 the chipped gear is in meshing, 2 the broken gear is in meshing, and 3 both the chipped and the broken gears are in meshing. It can be seen that the regularization dimensions of the faulty gearbox vibration signals are different from that of the healthy one. The difference of the regularization dimension between damage degrees 1 and 0, as well as that between damage degrees 2 and 1, is not very big, but it is relatively distinct between damage degrees 3 and 2. Most of all, with increasing damage degree, regularization dimension increases monotonically.

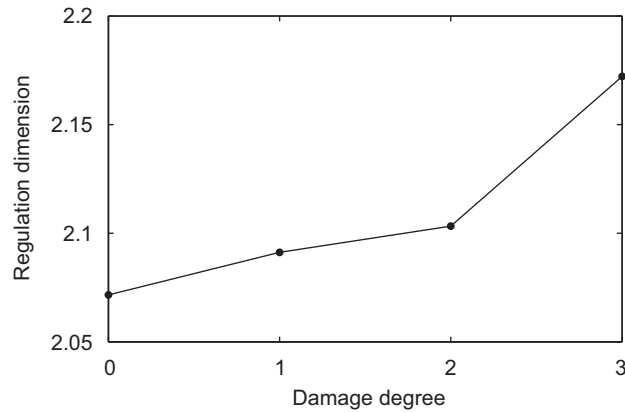


Fig. 8. Regularization dimension versus gear damage degree.

Table 5

Parameters in state space reconstruction of signals.

Gear condition	Normal	Chipped	Broken	Chipped and broken
Embedding dimension	4	4	5	4
Intra-vector spacing/time delay	2	2	2	2
Inter-vector spacing	1	1	1	1

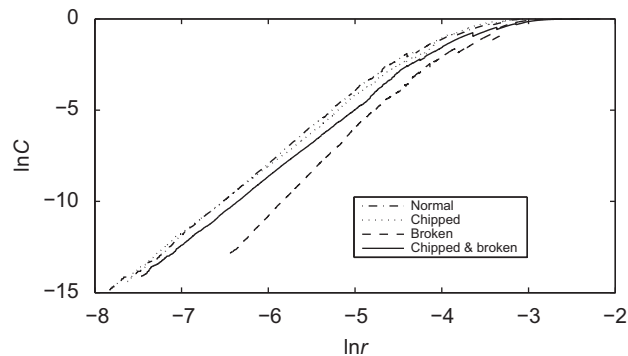


Fig. 9. Graph of $\ln C - \ln r$.

3.1.4. Comparison with correlation dimension and kurtosis

For comparison, the raw gearbox vibration signals are analyzed by means of correlation dimension and kurtosis. Correlation dimension is one of the most commonly used fractal dimensions. Its algorithm has been well developed, and is suitable to compute the fractal dimension of time series (signals). Therefore, it has been used to indicate the health status of bearings, gears, and rotating machinery [6–11]. Kurtosis characterizes the non-Gaussianity of signals. As a dimensionless statistic metric, it is insensitive to the amplitude and frequency variation of signals due to the inevitable instantaneous changes in machine-running conditions such as speed and load. It is widely used as an indicator for monitoring and diagnosis of machinery [1].

Following the procedure given in [7,8], the correlation dimensions of the same set of vibration signals are calculated. The parameters in state space reconstruction of signals are listed in Table 5. The logarithm of the correlation sum $\ln C$ versus the logarithm of the distance $\ln r$ is shown in Fig. 9. In the range $\ln r < -4.5$, the graph of $\ln C - \ln r$ has a linear trend. This means that the graph is nearly scale independent in this range, so it is used to compute the correlation dimension. By means of least squares error linear regression, a line can be found to fit each graph of $\ln C - \ln r$ in the range $\ln r < -4.5$, as shown in Fig. 10, and its slope equals the correlation dimension. The correlation dimensions of the gearbox vibration signals under the four conditions are listed in Table 4, and their variation versus the damage degree is shown in Fig. 11. The correlation dimensions of the faulty gearbox vibration signals are different from that of the healthy one, while unfortunately, they do not change monotonically with increasing damage degree. This is possibly due to noise interference by the bearing

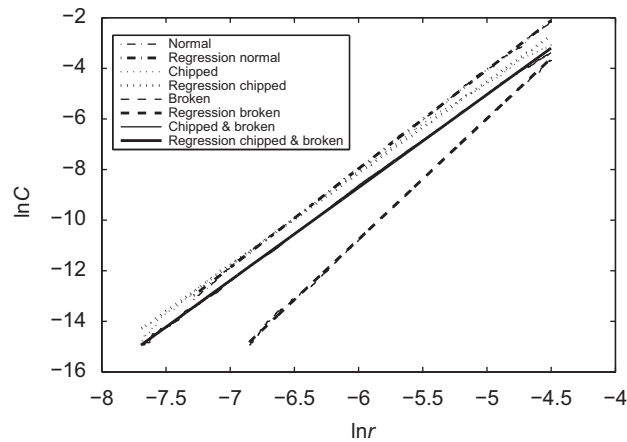


Fig. 10. Least squares regression.

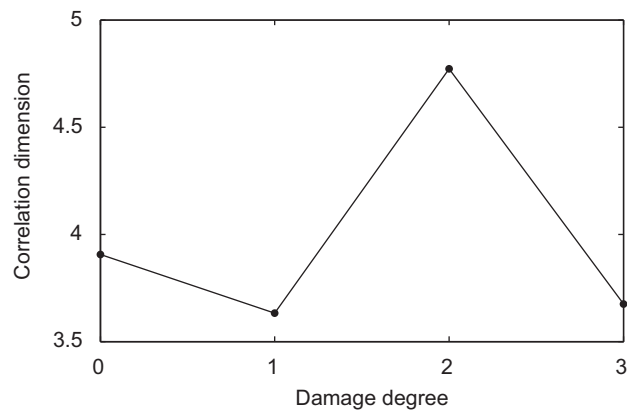


Fig. 11. Correlation dimension versus gear damage degree.

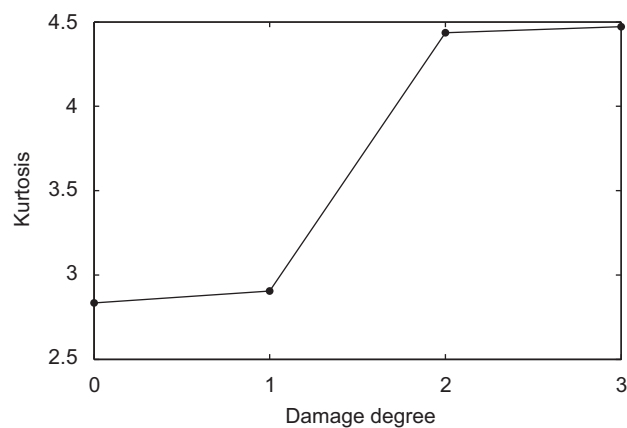


Fig. 12. Kurtosis versus gear damage degree.

vibration. The bearing vibration noise contaminates gear vibration signals, and may change the complexity of signals, so that the correlation dimension of the signals cannot reveal the real damage degree of the gears. In this sense, correlation dimension is not so effective as regularization dimension in assessing the gear damage degree.

The evolution of the vibration signal kurtosis with gear damage degree is shown in Fig. 12. The kurtosis of the normal gear and chipped gear vibration signals equal approximately 3, and this means that the signals are nearly Gaussian processes. The kurtosis of the broken gear and combined damaged gear vibration signals are larger than 3, which equal

approximately 4.5, and this means that the signals are non-Gaussian processes. The kurtosis increases monotonically with increasing damage degree, and the change from chipped gear to broken gear is significant, but the difference between the chipped gear and normal gear, as well as that between the combined damaged gear and broken gear, is relatively small, so it is not easy to differentiate the chipped gear damage from the normal gear, and the combined gear damage from the broken gear damage. Thus, it is not as effective as the regularization dimension.

3.2. Gear deterioration assessment

During the running of a gear, its health status deteriorates gradually. As a result, progressive damage will occur and ultimately result in sudden failure. In this section, vibration signals of a gearbox during a run-to-failure experiment are analyzed to further illustrate the performance of regularization dimension.

3.2.1. Specification of experimental system

Two pairs of gears are used to conduct the lifetime experiment in a limited time [17]. The experimental system, as shown in Fig. 13, is similar to that in Section 3.1.1 except for some minor modifications: the input shaft is driven by the motor through a pulley belt of ratio 4.2, and only one accelerometer is used and mounted on the middle of the gearbox side casing to collect vibration signals. The specification of gear teeth number is listed in Table 6.

The input shaft, shaft 1, is driven by the motor through the pulley belt at a speed of 2400 rpm, and the output shaft, shaft 3, is applied with a load of 40 Nm by the brake. The characteristic frequencies of shafts, gears, and rolling element bearings are summarized in Tables 7 and 8, respectively.

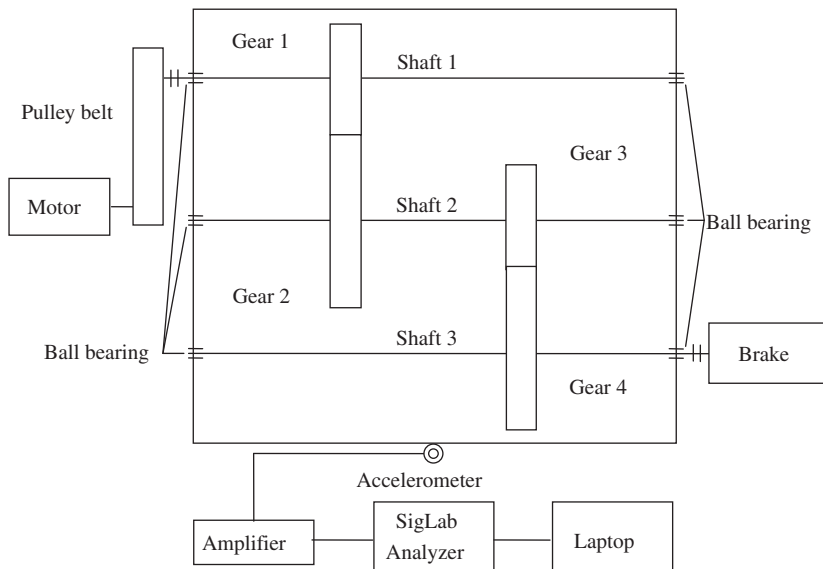


Fig. 13. Gearbox experimental system.

Table 6

Specification of gears.

Gear	1	2	3	4
Number of teeth	16	48	96	160

Table 7

Characteristic frequencies of shafts and gears.

Rotating frequency of shaft 1	Rotating frequency of shaft 2	Rotating frequency of shaft 3	Meshing frequency of gears 1 and 2	Meshing frequency of gears 3 and 4
9.52 Hz	3.17 Hz	1.90 Hz	152.32 Hz	304.00 Hz

Table 8

Characteristic frequencies of rolling element bearings.

Bearing supporting	Ball pass frequency inner race (Hz)	Ball pass frequency outer race (Hz)	Fundamental train frequency (Hz)	Ball spin frequency (Hz)
Shaft 1	76.332	43.610	6.230	58.134
Shaft 2	25.417	14.521	2.074	19.358
Shaft 3	15.234	8.704	1.243	11.602

**Fig. 14.** Photo of the damaged gear at the end of the experiment.

The vibration signals are collected at a sampling frequency of 5120 Hz once every 1 h, and 8192 points of data are recorded for each dataset. The signals in each dataset last 1.6 s, which covers 15.2 revolutions of shaft 1, 5.1 revolutions of shaft 2, and 3.0 revolutions of shaft 3. Therefore, the signals are long enough to investigate the gearbox dynamics.

The experiment had been running for 35 h, when the output shaft 3 stopped, and failures were found: gears 3 and 4 out of mesh, severe damage such as teeth bending, and breakage on gears 3 and 4 (as shown in Fig. 14).

In the following sections, 8 datasets that cover the continuous 8 h prior to the stop of shaft 3 are analyzed.

3.2.2. Spectral analysis

Waveforms and power spectra of the gearbox vibration signals are illustrated by four selected datasets, as shown in Fig. 15. Prior to the experiment, the range of vibration amplitude to be experienced was unknown. Hence the amplifier coefficient was set at the lowest to ensure the vibration signals to be within the range of the measurement system, even when the strongest vibration was experienced. So the magnitude of the collected signals is very small. For such signals, the limited precision in the process of data acquisition, storage, and visualization have caused the signal waveforms to appear to be not very smooth. Prior to the stop of the output shaft 3, the gear pair 3/4 deteriorated and tended to run out of mesh gradually. This means the engaging area was becoming progressively smaller along the gear facewidth, and the power that could be effectively transmitted to the output shaft 3 was also becoming progressively smaller. So the vibration amplitude of the signals shown in Figs. 15(b)–(d) is smaller than for those shown in Fig. 15(a).

From the power spectra, it can be seen that most of the signal energy is distributed in the frequency band 145–600 Hz. Among the four prominent peaks, the most significant two correspond to 223 and 446 Hz. They are possibly induced by the vibration of bearings, because they approximately equal the compound frequency of the shaft rotating frequency and harmonics of the bearing characteristic frequencies (e.g., $4 \times 58.134 - 9.52 = 223.016$ and $10 \times 43.610 + 9.52 = 445.52$ Hz. Refer to Table 8 for characteristic frequencies of the bearings). The other two appear at 149 and 298 Hz, which equal approximately the meshing frequencies of the two gear pairs.

3.2.3. Regularization dimension analysis

When computing the regularization dimensions with the FracLab toolbox, the Gaussian derivative order is fixed to $n=1$, the attenuation coefficient is set to the default value $\alpha=2$, and the time support i ranges from 2 to 52, i.e. $i=2, 3, \dots, 52$. According to Eqs. (6) and (7), the spectral mode center of corresponding Gaussian kernels ranges from 68.6 to 3497.4 Hz, so that all the major frequency components are covered.

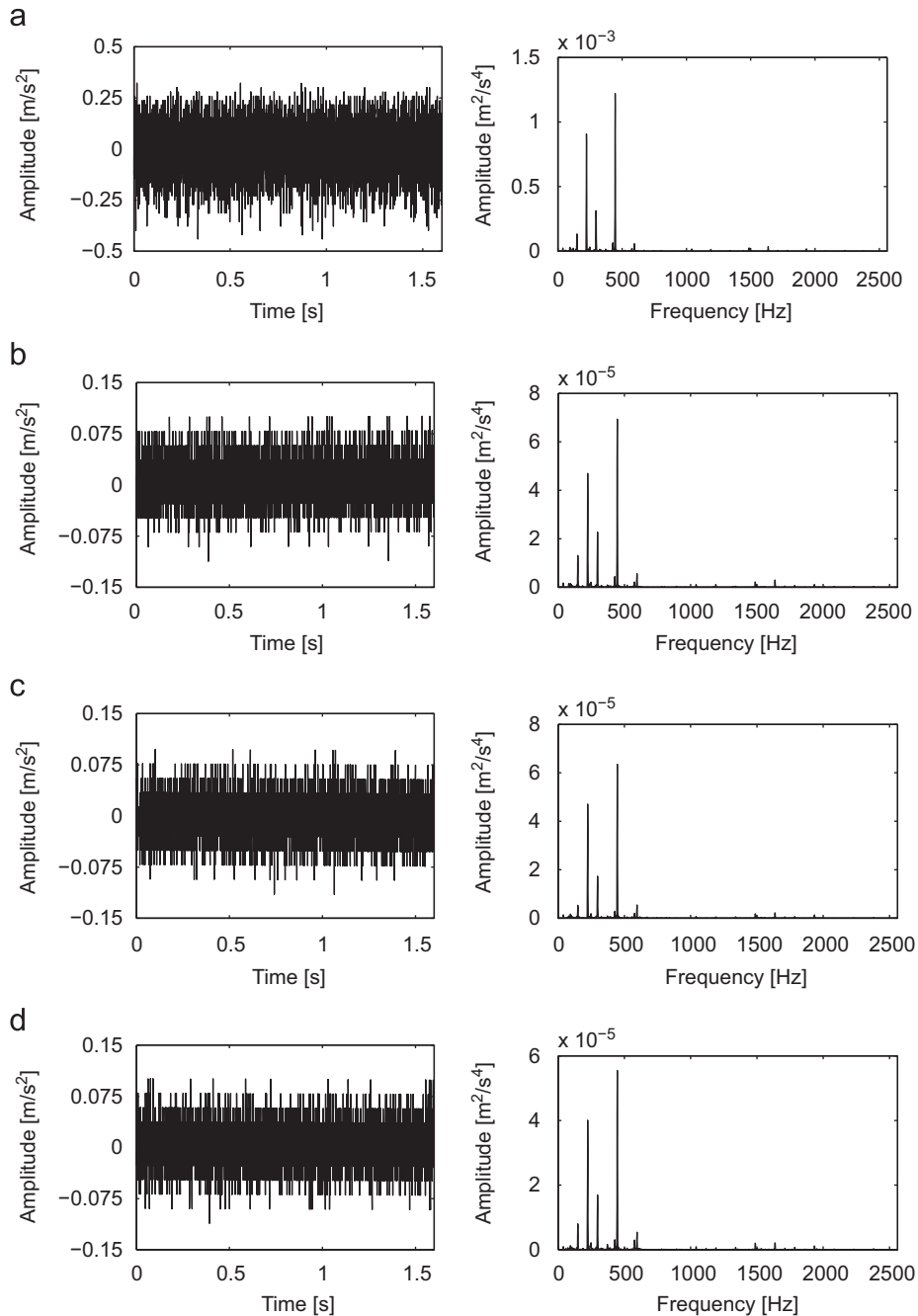


Fig. 15. Gearbox vibration signal waveforms (left) and power spectra (right): (a) 28th hour; (b) 30th hour; (c) 32nd hour; and (d) 34th hour.

The logarithm of the signal length $\ln l_\sigma$ versus the logarithm of the Gaussian kernel width $\ln \sigma$ is shown in Fig. 16. The graph of $\ln l_\sigma - \ln \sigma$ is nearly piecewise linear in some ranges, e.g., in the range $[0.1527, 1.2513]$ and $[1.2513, 2.0090]$ for $\ln \sigma$, the graph of $\ln l_\sigma - \ln \sigma$ has a linear trend and is nearly scale independent.

Since the failure and damage occurred on gears 3 and 4, the frequency band around their meshing frequency contains the information most useful to investigate the gearbox health status. So the almost scale-independent range $[0.6227, 1.1823]$, which corresponds to the time support $i=9,10,\dots,15$, frequency band 249.8–437.2 Hz, and covers frequency components only around the meshing frequency of gears 3 and 4, is used to compute the regularization dimension.

The other ranges that also have almost linear trend are not used, because their corresponding frequency bands do not cover any prominent components relevant to the gear health status.

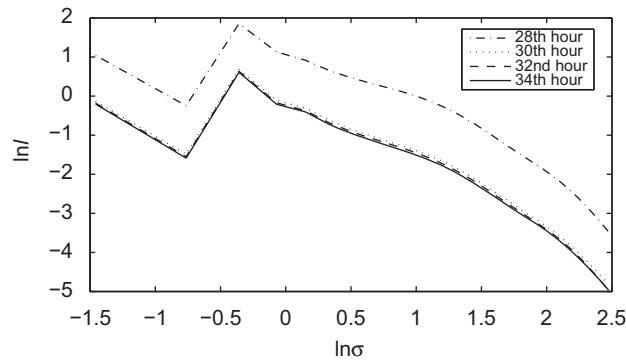


Fig. 16. Graph of $\ln l - \ln \sigma$.

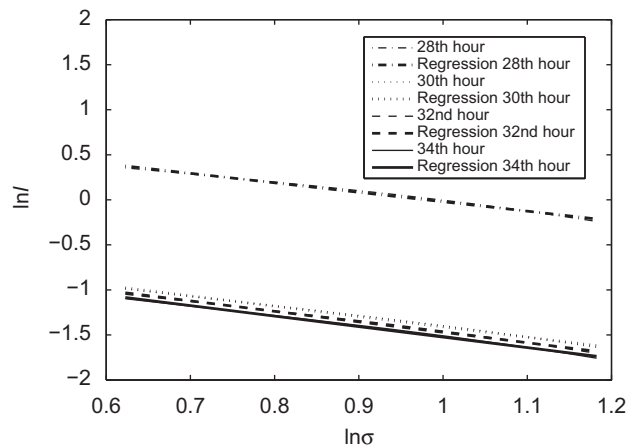


Fig. 17. Least squares regression.

Table 9
Fractal dimensions and kurtosis.

Running hour	28	29	30	31	32	33	34	35
Regularization dimension	2.0499	2.0806	2.1455	2.1533	2.1606	2.1741	2.1670	2.1905
Correlation dimension	3.7960	4.8100	3.9373	3.7044	4.0073	4.1955	3.6993	4.4188
Kurtosis	2.9687	2.8246	3.1028	2.7405	3.4438	3.9141	3.8725	3.7619

By means of least squares error linear regression, a line is found to fit each graph of $\ln l_\sigma - \ln \sigma$ in this range, as shown in Fig. 17. Regularization dimensions of the gearbox vibration signals are listed in Table 9, and their variation along the running hour is shown in Fig. 18. At the 34th hour, the regularization dimension is somewhat smaller than at the 33rd hour, but the difference is not very large and it is larger than those before and at the 32nd hour. This is possibly due to the experimental condition, measurement precision, and computational error. At the 29th hour, the regularization dimension shows a significant change. This indicates that the gearbox dynamic system becomes more complicated due to the deterioration, and the change in health status is early detected by regularization dimension. With increasing deterioration degree, the global trend of regularization dimension along running hour increases monotonically. In summary, the regularization dimension reveals the gearbox deterioration status.

3.2.4. Comparison with correlation dimension and kurtosis

For comparison, the raw gearbox vibration signals are also analyzed by means of correlation dimension and kurtosis.

The parameters in state space reconstruction of signals are listed in Table 10. The logarithm of the correlation sum $\ln C$ versus the logarithm of the distance $\ln r$ is shown in Fig. 19. In the range $-7.5 < \ln r < -6.6$, the graph of $\ln C - \ln r$ for each signal has a linear trend. This means that the graph is nearly scale independent in this range, so it is used to compute correlation dimension. By means of least squares error linear regression, a line is found to fit each graph of $\ln C - \ln r$ in the

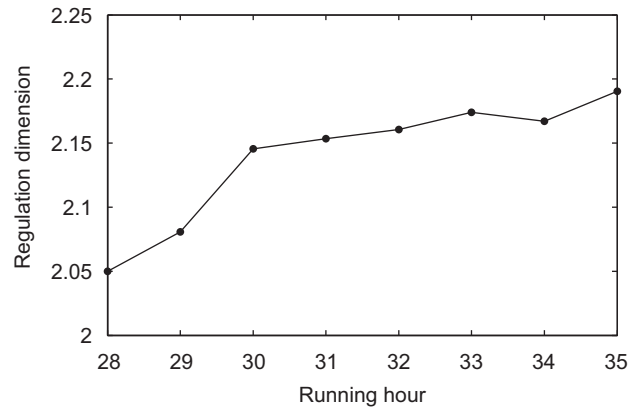


Fig. 18. Regularization dimension evolution.

Table 10

Parameters in state space reconstruction of signals.

Running hour	28	29	30	31	32	33	34	35
Embedding dimension	4	7	8	7	8	9	8	9
Intra-vector spacing/time delay	4	4	4	4	4	4	4	4
Inter-vector spacing	1	1	1	1	1	1	1	1

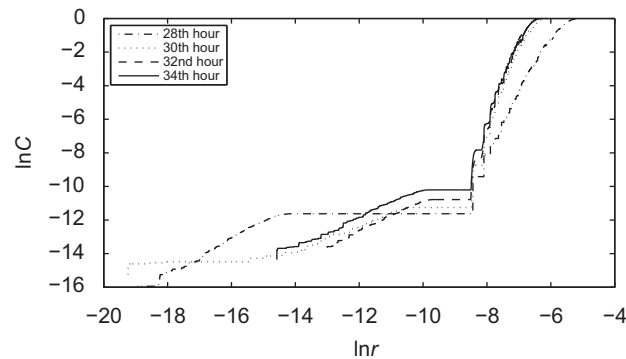


Fig. 19. Graph of $\ln C - \ln r$.

range $-7.5 < \ln r < -6.6$, as shown in Fig. 20, and its slope equals the correlation dimension. The correlation dimensions of the gearbox vibration signals are listed in Table 9, and their variation versus running hour is shown in Fig. 21. It can be seen that the correlation dimension does not increase or decrease monotonically along the running hour, i.e. the correlation dimension does not reveal the deterioration status of the gearbox. This can be attributed to the noise interference caused by the bearing vibration. This verifies again that correlation dimension is subject to many factors, especially noise interference and selection of scale-independent range.

The evolution of the vibration signal kurtosis with running hour (hours 28–35) is shown in Fig. 22. During the first 4 h (hours 28–31), the kurtosis of the gear vibration signals equals approximately 3, which means that the signals are nearly Gaussian processes. During the last 4 h (hours 32–35), the kurtosis of the gear vibration signals is larger than 3, but the difference from 3 is somewhat not large enough to indicate that the signals do not follow Gaussian processes any more. It seems that the change in the gearbox health status can be detected by kurtosis, but the relatively significant change is found at and after the 29th hour that a turning point is found through the regularization dimension. In this sense, kurtosis is not as effective in early detection of gear deterioration as the regularization dimension. Moreover, kurtosis does not change monotonically along the running hour, and this also makes it inferior to the regularization dimension.

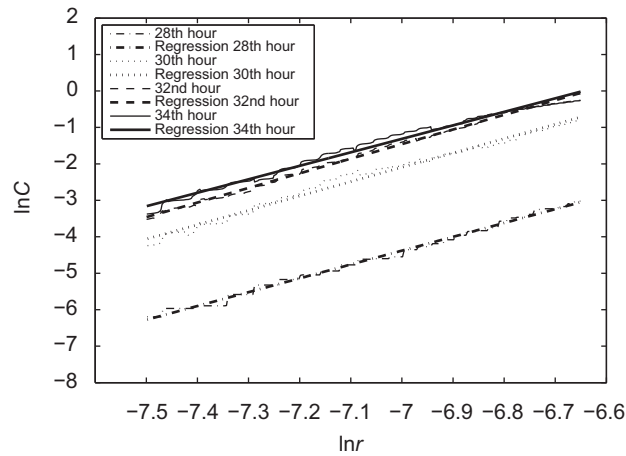


Fig. 20. Least squares regression.

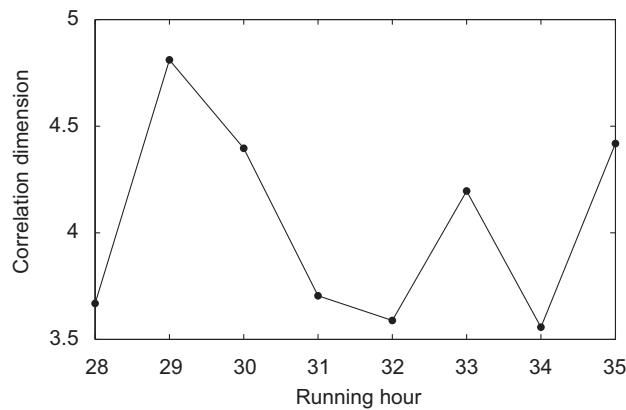


Fig. 21. Correlation dimension evolution.

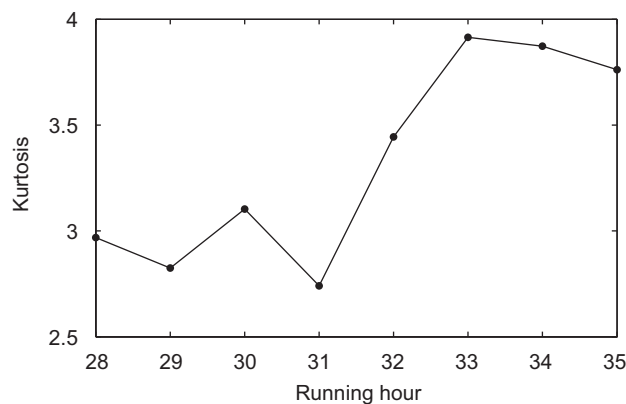


Fig. 22. Kurtosis evolution.

3.3. Discussion

Fractal dimension characterizes the complexity of a dynamic system. From the viewpoint of complexity, if a gearbox deteriorates or has a fault, it means that more factors get involved in the gear vibration, and the dynamic system becomes more complicated. Therefore, the fractal dimension of faulty gearbox vibration signals is expected to become larger than

that of healthy one. When only the chipped gear or the broken gear is in meshing, a single fault will induce extra vibration; as a result, the gearbox vibration becomes more complicated than when all the normal gears are in meshing, so the regularization dimension increases, although the increment is small. When both the chipped gear and the broken gear are in meshing, the compound fault induces much more extra vibration; as a consequence, the gearbox vibration becomes even more complicated, and the increment of regularization dimension is relatively significant. Similarly, during the running prior to failure or breakdown of a gear, its health status deteriorates, and the gearbox vibration becomes more complicated than that when the gear is normal, so the regularization dimension increases along the running hour.

The computational precision of correlation dimension depends on many factors, especially noise interference and selection of scale-independent range. Any inevitable noise in signals may cause an estimate error of correlation dimension. Although denoising may help in removing or suppressing the interfering noise, it may also cause loss of useful information, so that the correlation dimension after denoising may not be the real one. Another shortcoming is the absence of any criterion to select the scale-independent range when computing correlation dimensions. In most cases, the logarithm of correlation sum $\ln C$ versus the logarithm of distance $\ln r$ is piecewise linear, i.e. there may be multiple scale-independent ranges. Without a criterion, it is hard to determine which scale-independent range represents the real fractal dimension.

Kurtosis measures the non-Gaussianity of a signal. It is useful to differentiate a faulty gearbox from a healthy one, but it is not as effective as regularization dimension to assess the gear damage degree.

Overall, regularization dimension outperforms correlation dimension and kurtosis, and it is a potential tool for monitoring and diagnosis of gearboxes.

4. Conclusions

The regularization of a signal with Gaussian kernels is equivalent to filtering the signal with Gaussian filters. This provides a guide to select the scale-independent range for computing the regularization dimension. By properly selecting the parameters of Gaussian kernels, it enables one to focus on the signal components in a frequency band of interest without any preprocessing, and thereby to reveal the real condition of a machine using the regularization dimension.

The regularization dimension of the experimental gearbox vibration signals increases monotonically with increasing gear damage degree. This accords with the nature of a nonlinear dispersive dynamic system: the more severe the fault, the more complicated the dynamic system, and accordingly the larger the fractal dimension. These findings show the performance of regularization dimension in assessing localized gear damage.

Acknowledgments

This work is supported by the Natural Sciences and Engineering Research Council of Canada, the National Natural Science Foundation of China (50705007), and the Scientific Research Foundation for Returned Overseas Chinese Scholars, Ministry of Education, China. The regularization dimensions are computed using the software FracLab developed by INRIA France. Thanks also go to the anonymous reviewers for suggestions, which were very helpful in our revision of this paper.

References

- [1] P.D. Samuel, D.J. Pines, A review of vibration-based techniques for helicopter transmission diagnostics, *Journal of Sound and Vibration* 282 (1–2) (2005) 475–508.
- [2] B.B. Mandelbrot, *The Fractal Geometry of Nature*, W.H. Freeman, San Francisco, 1982.
- [3] K. Falconer, *Fractal Geometry: Mathematical Foundations and Applications*, second ed., Wiley, Chichester, 2003.
- [4] K. Falconer, *The Geometry of Fractal Set*, Cambridge University Press, Cambridge, 1985.
- [5] F.C. Moon, *Chaotic Vibrations: An Introduction for Applied Scientists and Engineers*, Wiley, New York, 1987.
- [6] B.Q. Shi, Y.H. Shen, *Fractal Approach to Fault Diagnosis of Machinery: Principles and Applications*, Metallurgical Industry Press, Beijing, 2001 (in Chinese).
- [7] D. Logan, J. Mathew, Using the correlation dimension for vibration fault diagnosis of rolling element bearings-I: basic concepts, *Mechanical Systems and Signal Processing* 10 (3) (1996) 130–149.
- [8] D. Logan, J. Mathew, Using the correlation dimension for vibration fault diagnosis of rolling element bearings-II: selection of experimental parameters, *Mechanical Systems and Signal Processing* 10 (3) (1996) 251–264.
- [9] J.D. Jiang, J. Chen, L.S. Qu, The application of correlation dimension in gearbox condition monitoring, *Journal of Sound and Vibration* 223 (4) (1999) 529–541.
- [10] W.J. Wang, J. Chen, X.K. Wu, Z.T. Wu, The application of some non-linear methods in rotating machinery fault diagnosis, *Mechanical Systems and Signal Processing* 15 (4) (2001) 697–705.
- [11] J.Y. Yang, Y.Y. Zhang, Y.S. Zhu, Intelligent fault diagnosis of rolling element bearing based on SVMs and fractal dimension, *Mechanical Systems and Signal Processing* 21 (5) (2007) 2012–2024.
- [12] F. Roueff, J. Lévy Véhel, A regularization approach to fractional dimension estimation, in: *Proceedings of Fractals 98*, Malta, October 1998.
- [13] J. Lévy Véhel, P. Legrand, Signal and image processing with FracLab, in: *Proceedings of Fractal04, Complexity and Fractals in Nature*, Eighth International Multidisciplinary Conference, Vancouver, Canada, April 4–7, 2004.
- [14] J.A. Bloom, T.R. Reed, A Gaussian derivative-based transform, *IEEE Transactions on Image Processing* 5 (3) (1996) 551–553.
- [15] S. Karmakar, K. Ghosh, R.K. Saha, S. Sarkar, S. Sen, A new design of low pass filter by Gaussian derivative family, in: *Proceedings of the Third International Conference on Intelligent Sensing and Information Processing*, December 14–17, 2005, pp. 177–182.
- [16] X. Tian, J. Lin, M. Agelinchaab, J. Zhang, M. Akhtar, M.J. Zuo, K.R. Fyfe, Experiment 02-05 on gearbox, Technical Report, University of Alberta, 2002.
- [17] X.F. Fan, H. Lin, M.J. Zuo, Gearbox lifetime assessment experiment, Technical Report, University of Alberta, 2004.